Colloid Polym Sci 276:920–929 (1998)

ORIGINAL CONTRIBUTION

D. Duracher
F. Sauzedde
A. Elaïssari
C. Pichot
L. Nabzar

Cationic amino-containing *N*-isopropylacrylamide-styrene copolymer particles: 2-surface and colloidal characteristics

Received: 20 January 1998
Accepted: 8 June 1998

D. Duracher · F. Sauzedde · A. Elaïssari
C. Pichot (✉)
Ecole Normale Supérieure de Lyon
CNRS-bioMérieux
46 Allée d'Italie
F-69364 Lyon
France
E-mail: Christian.Pichot@ens-bma.cnrs.fr

L. Nabzar
ICS
6 Rue Boussingault
F-67083 Strasbourg Cedex
France

Abstract In a previous paper [1], the synthesis of various polystyrene–poly[NIPAM] core–shell latexes bearing cationic amidino and/or amino charges has been described. Several colloidal properties of these cationic latexes have been characterized such as: particle size, surface charge density, electrophoretic mobility and finally colloidal stability. Due to the poly[NIPAM]-rich layer in the shell, it was found that temperature played a significant role on all these properties, a LCST around 33 °C being exhibited. In addition, ionic strength was also found to affect the colloidal behavior of these latexes, the largest effect being observed with latexes having both amidino and amino surface charges. The critical coagulation concentrations (CCC) of the various latexes above and below the LCST were determined, highlighting the contribution of electrostatic and steric repulsive forces to the stability of these particles.

Key words Poly(styrene/*N*-isopropylacrylamide) latexes – particle size – electrokinetic properties – colloidal stability

Introduction

In the past decade, stimuli-responsive particles have received increasing attention due to their outstanding properties explaining their potential interest in many applications [2–6]. For that purpose, polymeric colloids containing *N*-isopropylacrylamide moieties have appeared quite suitable and their synthesis is now well documented [7–10]. A large amount of work has been developed on the thermal sensitivity of poly[NIPAM] exhibiting a lower critical solubility temperature (LCST) in the temperature range 30–35 °C. Such a property was found appropriate for the separation of biomolecules, motivating the use of poly[NIPAM] in biology either as a support for antibodies (immunoassay tests, for instance) or in drug delivery systems. Moreover, these hydrophilic polymer colloids also attracted much academic interest as regards to their colloidal behavior [8, 11–17] under various adverse conditions of temperature, salinity and pH.

Due to the large swelling capacity of poly[NIPAM]-based latexes in water, a dramatic decrease of the particle size occurred above the LCST as well evidenced by Pelton et al. [11] Kawaguchi et al. [3] and Snowden et al. [12]. The first authors [11, 14] also showed that electrokinetic properties of such hydrogel latexes were sensitive to both the temperature and ionic strength. It was reported that the electrophoretic mobility of the poly[NIPAM] particles increased upon increasing the temperature above the LCST. Such a behavior was explained by an increase in the surface charge density when the particle size decreased.

Moreover, the effect of salinity on the electrophoretic mobility of these hydrophilic particles has been thoroughly examined by Ohshima et al. [15, 16], who proposed a theory based on Varoqui's concept [18] by taking into account the charge density, the friction factor and the shear plane position as a function of ionic strength. The proposed theory [16] was found to be in good agreement with experimental data for polystyrene particles covered by poly[*N*-isopropylacrylamide] shell irrespective of temperature. In addition, no maximum in the electrophoretic mobility versus ionic strength was observed whatever the temperature (above and below the LCST) [16], unlike what was reported in the case of hydrophobic particles bearing an hairy layer [19]. The LCST was found to be dependent on the hydrophilic/hydrophobic property and charge nature of the comonomer as reported by Priest et al. [20] and Chen at al. [21], respectively. However, to our knowledge, there was no systematic study investigated on the colloidal stability behavior of these thermosensitive particles as a function of temperature.

In a previous paper [1], we already reported the synthesis of various monodisperse cationic polystyrene/poly [NIPAM]core–shell latexes either by batch emulsifier-free emulsion copolymerization or by a two-steps process using aminoethyl methacrylate hydrochloride (AEM) as a comonomer, methylenebisacrylamide as crosslinker and 2,2′ azobis(2-amidinopropane)dihydrochloride as initiator. It was particularly emphasized that the build-up and structure of the hydrophilic shell layer were very much dependent upon the polymerization process and amount of AEM used.

In this paper, we aimed at describing several colloidal properties of these cationic polystyrene/poly[NIPAM] core–shell latexes. The dependence of particle size, electrophoretic mobility and colloidal stability on temperature and ionic strength has been successively investigated and discussed.

Experimental section

Materials

Sodium chloride (NaCl) was used as received for ionic strength variation, DL-dithiothreitol (DDT) (from Sigma), 3-(2-pyridyldithio)-propionic acid *N*-hydroxysuccinimide ester (SPDP) (from Sigma) and 4-dimethylaminopyridine (DMAP) (from Aldrich) were used for amino group titration. Well-deionized and deoxygenated water (Milli-Q water, Millipore system) was used in all preparations.

Preparation of latexes

The cationic amino containing *N*-isopropylacrylamide–styrene copolymer latexes were synthesized using emulsifier-free emulsion polymerization. A detailed kinetic study on the polymerization of such systems (styrene, *N*-isopropylacrylamide) and (styrene, *N*-isopropylacrylamide, aminoethylmethacrylate) has been given in a previous paper [1].

All the latexes were cleaned by repetitive centrifugation using deionized Milli-Q water, before any characterization study, in order to remove free electrolytes and water soluble polymers.

Characterization of latexes

Particle size determination

Latex particle size was measured by quasi-elastic light scattering (QELS) as a function of temperature (from 20 to 50 °C) using an N4MD apparatus from Coultronics, France. The mean hydrodynamic diameter was calculated from the diffusion coefficient measurement, which, in the high dilution limit of negligible particle–particle interactions, is calculated by using the Stokes–Einstein equation [22].

$$D = \frac{kT}{3\pi\eta D_h}, \qquad (1)$$

in which D is the diffusion coefficient, k the Boltzmann constant, T absolute temperature, and η the viscosity of the medium. Particle size was also measured using transmission electron microscopy (TEM) (from Philips) at room temperature by sizing about 50 particles, allowing the determination of the number ($\overline{D_n}$), weight ($\overline{D_w}$), average diameter and the polydispersity index (PDI $= \overline{D_w}/\overline{D_n}$).

Surface charge density

Surface charge density was determined by colorimetric titration using the SPDP method [23]. This method relies on the chemical reaction of the *N*-hydroxysuccinimide of 3-(2-pyridyldithio)-propionic acid *N*-hydroxysuccinimide ester (SPDP) with the primary amino and amidine groups located on the latex surface. The ultraviolet (UV) method was used for the quantitative estimation of pyridine-2-thione, allowing the quantification of the surface amino and amidine groups. The principle of the chemical reaction is illustrated in Scheme 1.

Electrophoretic mobility

The electrophoretic mobility of latex particles [24, 25] was measured with the Zeta Sizer III (from Malvern Instruments, England) as a function of pH, ionic strength (NaCl) and temperature. Each point is the average of at least five measurements.

Measurement of stability ratios

Critical coagulation concentration (CCC) was determined from the coagulation rate constants as a function of ionic

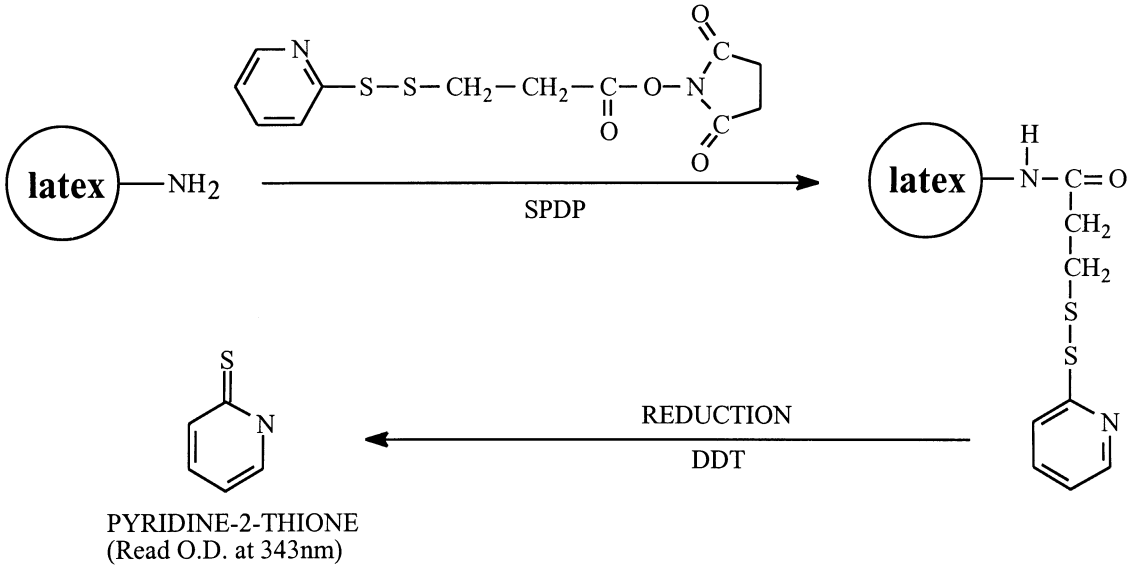

Scheme 1

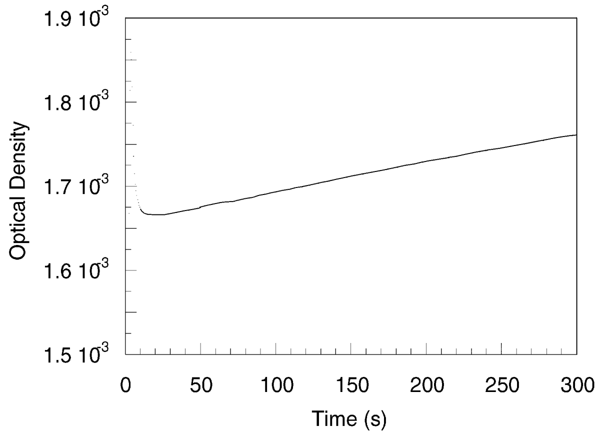

Fig. 1 Optical density versus time (*s*) for typical coagulation measurement using NaCl salt (at 20 °C)

strength (NaCl) and at two temperatures (20 and 43 °C). The optical density variation (Fig. 1) of the latex was first measured at a 600 nm wavelength by rapid mixing of the latex particles and the electrolyte solution, using a UVIKON 930 spectrophotometer. The turbidity variation versus time induced by the coagulation of latex particles can be obtained using the relationships between the optical density and the turbidity as given by the following equation:

$$\tau = 2.303 \frac{OD}{L} , \tag{2}$$

where OD is the optical density and L is the length of the sample (in cm).

The stability factor W [26] defined by Eq. (4) was obtained as the ratio of the initial slope of the turbidity versus time for fast (k_f) and slow (k_s) coagulation, respectively:

$$k_f = \left(\frac{\partial \tau}{\partial t}\right)_f , \quad k_s = \left(\frac{\partial \tau}{\partial t}\right)_s , \tag{3}$$

$$W = \frac{k_f}{k_s} . \tag{4}$$

The CCC was then obtained from the ionic strength concentration (C_s) (where C_s is the electrolyte concentration; NaCl) at which the slope ($\log(W)/\log(C_s)$) of $\log(W)$ versus $\log(C_s)$ variation was reduced to zero.

Results and discussion

All latexes prepared according to formulation recipes detailed in Ref. [1] were characterized with respect to particle size and size distribution, surface charge density, electrophoretic mobility and colloidal stability. For sake of clarity, the behavior of selected samples was reported to illustrate the variation of a specific colloidal property as a function of experimental parameters (pH, ionic strength and temperature).

Particle size and size distribution

At first, the latexes were examined by TEM as shown in Fig. 2 for four samples. It is worth mentioning that all

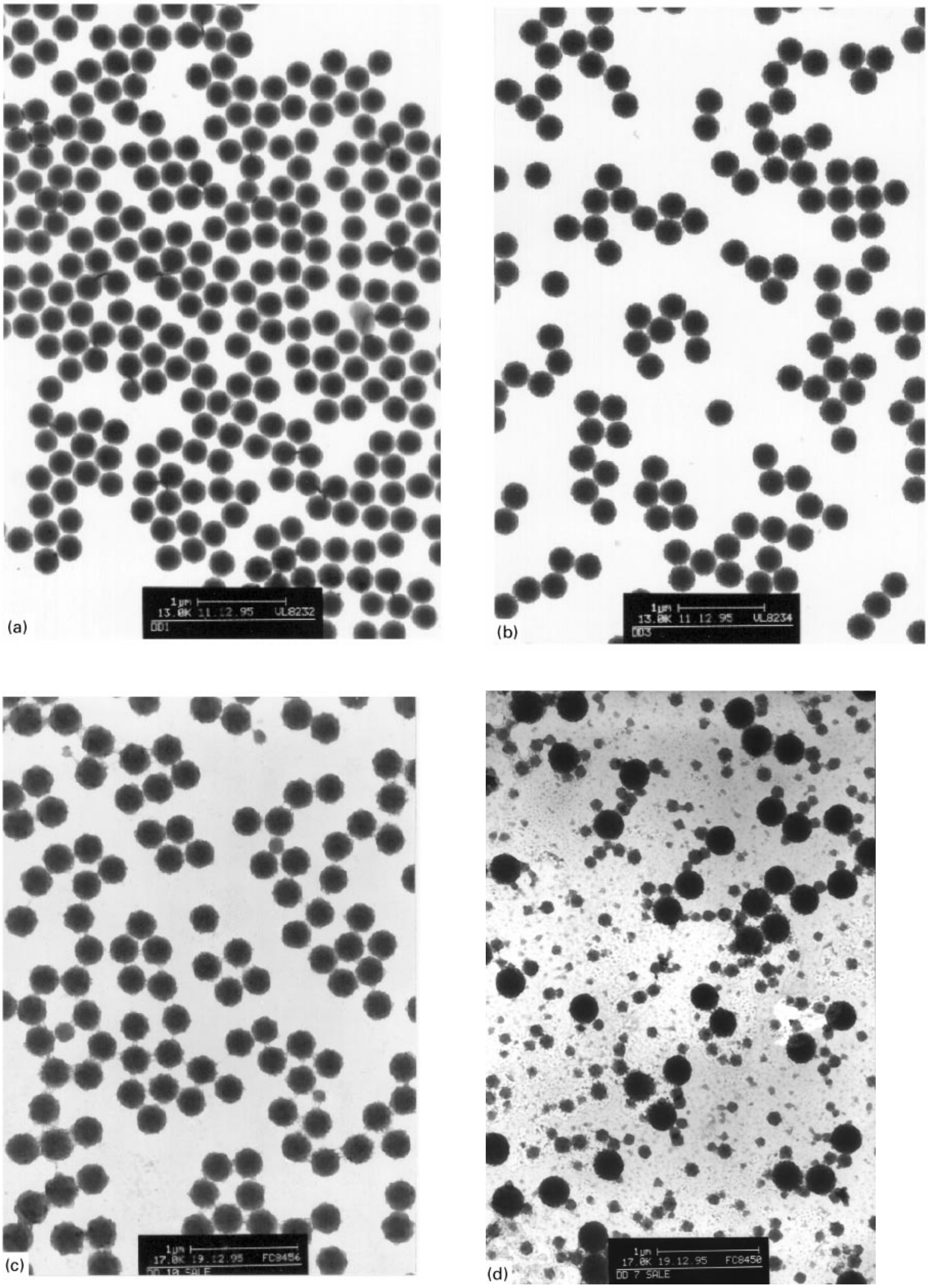

Fig. 2 Transmission electron micrographs of various latexes DD1 (a), DD3 (b), DD10 (c) and DD7 (d) samples

Table 1 Particle size D_h and D_{TEM} as determined by QELS and TEM, respectively

Sample	AEM[a) [%]	D_h (20 °C) [nm]	D_h (50 °C) [nm]	D_{TEM} [nm]	PDI[b)	δ[c) [nm]
DD1[d)	0 (batch)	356	310	306	1.007	23
DD3	2 at 57	573	352	321	1.047	110
DD4	2 at 89	551	358	303	1.011	96
DD5	2 at 94	595	385	315	1.010	105
DD6	2 at 97	580	364	335	1.008	108
DD7	2 at 31	*	*	*	*	*
DD10	0 at 70	603	364	288	1.012	119
DD12	3 at 70	484	334	302	1.004	75
DD11	4 at 70	358	315	303	1.005	21

[a) The percent of AEM added at a given conversion of seed polymerization.
[b) The polydispersity of latex particles from TEM.
[c) δ (nm) = $(D_{h,20°C} - D_{h,50°C})/2$.
[d) DD1 latex bearing amidine groups was prepared by batch soap-free emulsion polymerization (styrene, NIPAM and V50).
*) Polydisperse latex particles.

latexes exhibit a narrow size distribution except for sample DD7 in which the shot addition of the monomer mixture was performed at too low conversion. Such a result is the consequence of the mechanism of particle formation in this precipitation polymerization process leading to a constant number of particles early in the conversion as detailed in the previous paper [1]. As also evidenced from TEM data collected in Table 1, the average number particle size is around 300 nm, regardless of the synthesis process, an indication that the final hydrophilic particles are in a shrunken form in the dried state and appear spherical when viewed by TEM. Due to the complex nature of the shell of these particles, i.e. the presence of a thermosensitive polymer with cationic charges at chain ends or distributed along with the chain, a thorough study was investigated on the influence of both the temperature and ionic strength on the particle size.

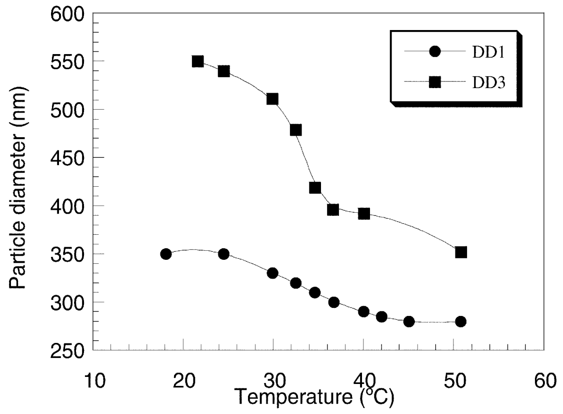

Fig. 3 Temperature dependence of the hydrodynamic size of DD1 and DD3 latexes at 10^{-3} M ionic strength (NaCl) and pH 6

Effect of temperature

Particle diameters were measured by dynamic light scattering in diluted dispersions. The hydrodynamic diameter of the particles, D_h, is the distance from the center of the particle to the shear plane at the surface, which is assumed to be that of a nondried particle.

The variation of the hydrodynamic diameter D_h as a function of temperature for two latexes (DD1 and DD3) is reported in Fig. 3. As expected, a remarkable change is observed around 32 °C which corresponds to the LCST of poly[NIPAM] [27, 28]. Particle size for both latexes appears constant below 27 °C and above 35 °C. However, in the temperature range (27–35 °C), particle size drastically decreases, due to the shrinkage of the shell containing poly[NIPAM], induced by dehydration of amide moieties in the hydrogel. The dehydration process leads to a coil–globule transition, a phenomenon which has been extensively investigated and discussed by several authors [11–13, 29].

Based on this preliminary study, particle size of all the latexes were then determined at 20 and 50 °C, respectively. The difference between the hydrodynamic diameters below and above the LCST of poly[NIPAM] provides a qualitative estimation of the hydrogel shell thickness (δ) (and consequently on the swelling property), as reported in Table 1 for various latexes. It is clearly evident that the core–shell latex particles prepared by batch polymerization in the absence of AEM and MBA exhibit a slighter thickness (δ) than those obtained with a two-step process (shot polymerization), probably due to the largest amount of NIPAM used in this latter process. In addition, the hydrogel thickness in core–shell latexes depends on both the AEM concentration introduced during the shot addition (DD10, DD12 and DD11) and the conversion of the initial batch polymerization at which the shot addition was performed. The effect of AEM seems more significant, a result which has been interpreted by a transfer reaction entailed by the amino-containing monomer and causing the production of large amounts of water soluble polymers [10].

Effect of ionic strength

Particle diameter (QELS) was then investigated as a function of monovalent electrolyte concentration (NaCl) and the results are given in Fig. 4 for two latex samples (DD1 and DD4). In both cases, the hydrodynamic diameter is found to decrease upon increasing the electrolyte concentration. The effect was more marked in the case of two-step polymerized sample (DD4) than with the batch one (DD1), containing a lesser amount of poly[NIPAM]. The influence of salinity on the hydrodynamic size variation can be explained by reference to the contribution of two phenomena:

- As reported by several authors [8, 30], increasing the electrolyte concentration was found to cause a decrease of the medium solvency of poly[NIPAM] (increase in the Flory–Huggins interaction parameter between the polymer and water) even below the LCST, then resulting in the reduction of the poly[NIPAM] coil volume.
- In the case of hairy particles in which the polymer chains at the particle surface are polyelectrolytes, adding salt (NaCl) screens the electrostatic repulsions between the ionic groups distributed along with the polyelectrolyte chains. This also results in a decrease of the hydrodynamic volume of the corresponding polyelectrolyte hairs as recently discussed by Seebergh et al. [31].

On this basis, it can be postulated that the first effect is probably more involved in the case of DD1 sample in which cationic groups are only located at chain ends. Contrarily, the second effect, and perhaps also the first one but at a lesser extent, would be more responsible for the reduction of the thickness layer in the case of shot-growth latexes (DD4).

A complex combination of both contributions dictates the stability, the equilibrium and the swelling state of such a hydrogel shell as a function of environmental conditions.

Surface charge density

The concentration of amino and amidine groups on the latex surface was determined by colorimetric titration as reported in the first column of Table 2 for all the latexes. The surface charges for batch latex particles only originate from the initiator fragments, whereas, for shot-growth latex particles, they come from both the initiator (V50) and the functional monomer (AEM). Since the ionic charges are more or less randomly distributed within the hairy layer, the surface charge density were only expressed in mole/g instead of mole/m^2.

Due to the use of a cationic monomer (AEM) in the preparation of shot-growth latexes, their surface charges are significantly higher than for the batch one. In addition, as expected, the charge density (in mole/g) is found to rise when the concentration of the functional monomer was increased during the shot process (DD1 to DD11 samples). These results corroborate that the best way to increase the incorporation yield of the functional monomer on this type of latex relies on the use of a two-step polymerization process.

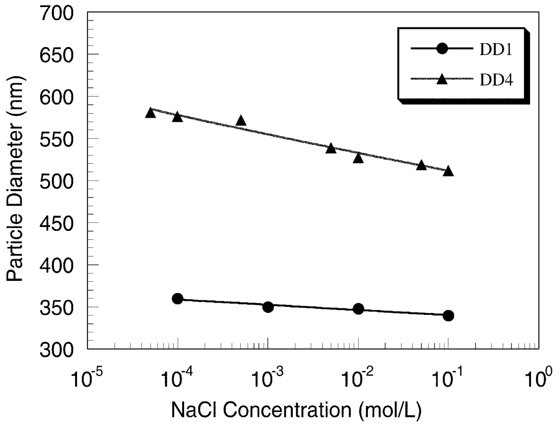

Fig. 4 Particle size as a function of ionic strength in semi log presentation for DD1 and DD4 latexes (pH 6.0, temperature 20 °C)

Table 2 Charge density (in μmole/g) and electrophoretic mobility (μ_e) at 20 and 40 °C for all latexes

Sample	σ [μmole/g]	μ_e at 20 °C[a] [10^{-8} m^2/Vs]	μ_e at 40 °C[a] [10^{-8} m^2/Vs]
DD1	12.30[b]	2.0	3.81
DD3	24.10	1.4	3.5
DD4	14.60	0.5	2.7
DD5	15.96	ND	ND
DD6	15.93	0.7	2.7
DD10	10.20[b]	0.5	3.8
DD12	35.00	1.7	ND
DD11	23.70	2.1	ND

ND = not determined.
[a] Measured at pH 6.0 and 10^{-3} ionic strength (NaCl).
[b] Latex particles bearing only amidine groups.

Electrophoretic mobility

The electrophoretic mobility (μ_e) measurements of these stimuli-responsive polymer colloids were investigated as a function of pH, and ionic strength and temperature, with a view to identifying the nature of the surface charge and the electrokinetic behavior of the various latexes in relation to their interface structure.

Effect of pH on the electrophoretic mobility

The electrophoretic mobilities (μ_e) of the latex particles were examined as a function of pH at a constant ionic strength (10^{-3} mole/l NaCl). The behavior of DD1, DD3 and DD11 samples was compared in order to highlight the effect of the polymerization method and composition of the recipe on the electrokinetic properties of the final latexes.

From Fig. 5, showing the variation of the electrophoretic mobility as a function of pH, it appears that all the latexes exhibit a positive mobility below pH 9 as expected from the nature of the cationic charges. As pH increases from 9 to 10, the electrophoretic mobility gradually decreases, revealing the partial neutralization of amidine and amine groups in this pH range. The isoelectric points (IEP) of these cationic core–shell latexes are found to be close to 10 for amidine latexes and 9.5 for amine ones. Similar data have already been reported in the case of polystyrene cationic latexes bearing amidine and/or amine groups (using AEM monomer) [32, 33]. The negative electrophoretic mobility observed above pH 10 is usually attributed to the presence of carboxylic groups originated from the hydrolysis of amidine groups [27].

Comparison of DD1 and DD3 samples allows to show the differences in the electrokinetic behavior between batch (amidine) and shot (amine and amidine) polymerized latexes. In the case of DD1, μ_e starts to gradually decrease at lower pH than with DD3 for which a plateau value prevails up to pH 9. Besides, comparison of DD3 and DD11 samples evidences the influence of the amount of the functional monomer (Table 1). It can be seen that DD11 sample with 4 mole% AEM exhibits a higher plateau (μ_e) value than DD3 which was obtained with only 2 mole%. As a general remark, there is no "linear" relationship between the surface charge density and the electrophoretic mobility at the plateau value (in the acidic range domain) as predicted by the theory [24]. This anomaly can be attributed to: (i) the complexity of the shell structure (cross-linking density, thickness layer, etc.), (ii) the surface morphology as pointed out in the previous paper [1] and (iii) the charge distribution in the hydrogel shell volume.

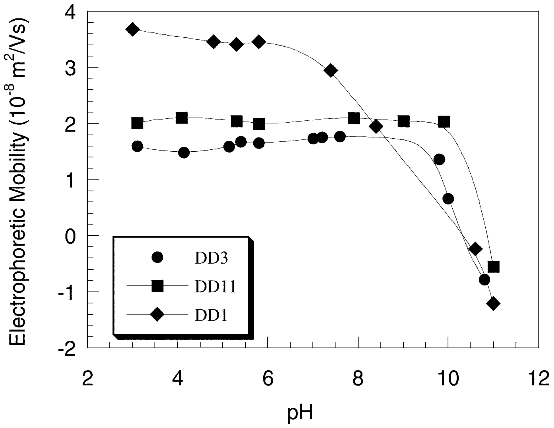

Fig. 5 Electrophoretic mobility of DD1, DD3 and DD11 latexes as a function of pH at a constant ionic strength 10^{-3} M and at 20 °C

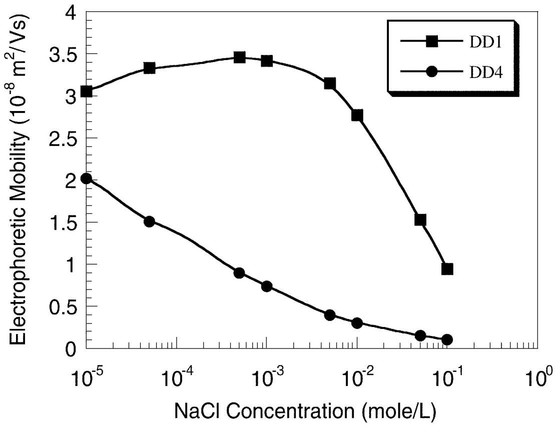

Fig. 6 Electrophoretic mobility of DD1 and DD4 latexes as a function of ionic strength at a constant pH 6.0 and at 20 °C

Effect of ionic strength

This was investigated at room temperature and pH 6 with DD1 and DD4 latexes, the results are illustrated in Fig. 6. For the batch latex (DD1), electrophoretic mobility versus ionic strength exhibits a marked maximum as clearly seen for negatively [33] or positively [34] polystyrene latexes. However, no maximum was observed in the case of the shot growth (DD4) latex, a behavior in quite good agreement with that already reported by Mc Phee et al. [8] and Makino et al. [16]. The presence or the absence of a maximum in the μ_e variation versus salinity of the medium, has been attributed to the surface particle structure of the latex investigated (smooth or hairy layer).

Tentative interpretation of such a variation in the electrophoretic mobility profile versus ionic strength of both latexes is questionable since several phenomena are simultaneous involved: (i) volume charge density; (ii) adsorption of co-ions; (iii) particle electrical conductance; (iv) thickness layer, concentration of polyelectrolytes chain and cross-linking density of the shell (in DD4).

Such a difference can be qualitatively explained by considering the nature of the shell whose structure is controlled by the mode of polymerization process performed for preparing the two latexes. In the case of DD1 sample (batch latex) it was previously evidenced [1] that particles resulted from a complex polymerization mechanism providing, after a phase separation step, a polystyrene-rich core surrounded by a poly[NIPAM]-rich shell. Although the compatibility of the two-polymer phase, is probably ensured by a small interphase of styrene–NIPAM copolymer chains, it may be suggested that such batch particles would behave like "hairy" particles. On the contrary, the shell of DD4 latex was built through shot-polymerization of a NIPAM, MBA, AEM mixture onto a polystyrene-rich seed. It should be remembered that the presence of the cross-linker results in the formation of a dense hydrogel shell in which the presence of long flexible hairs is strongly limited. Therefore, in spite of the complexity of the shell structure, these shot-growth particles behave more likely than "smooth" particles.

Effect of temperature

As illustrated in Fig. 7 for DD1, DD6 and DD11 samples, all latexes show positive electrophoretic mobilities irrespective of temperature from 20 to 40 °C. A general tendency is that μ_e increases when raising the temperature of the medium, with a magnitude depending upon the overall charge amount (see Table 2). This can be considered as a consequence of the shrinkage of the interfacial shell layer located on the latex, as shown in Fig. 3, in which particle size variation versus temperature was reported. When the temperature increased from 20 to 40 °C, the hydrodynamic diameter (D_h) decreased resulting in an increase in the surface charge density (σ) and consequently, an increase in the electrophoretic mobility (μ_e). This result can be explained by the following relationships [11] between surface charge density (σ) (5), particle size and electrophoretic mobility (6) as a function of temperature

$$\sigma = -\frac{Ne}{4\pi r^2}, \qquad (5)$$

$$\mu_e = -\frac{Ne}{4\pi\eta\kappa r^2}, \qquad (6)$$

where N is the number of cationic groups per particle, e is the electron charge, r is the hydrodynamic radius of the

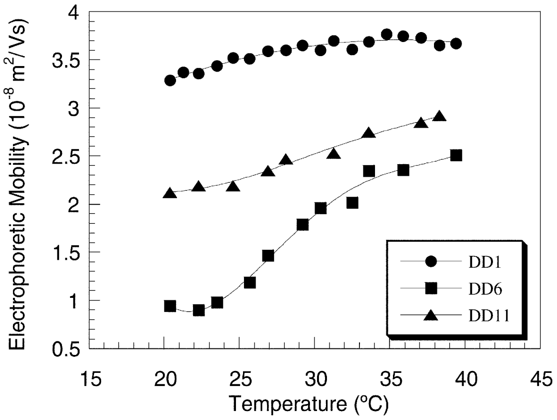

Fig. 7 Electrophoretic mobility of DD1, DD6 and DD11 latexes as a function of temperature at pH 6 and ionic strength 10^{-3} M

spherical particle, κ is the reciprocal Debye length thickness and η is the viscosity of the medium. The influence of temperature is less significant with DD1 sample than with DD6 and DD11 ones, which can be attributed to the following effects: (i) small hairy layer in DD1 with most of the charges located near the surface of the particles; (ii) a more thick shell layer in DD4 with charges distributed throughout the shell volume. The larger the shell layer containing poly[NIPAM] hydrogel, the more important is the influence of temperature, as already pointed by Pelton et al. [11] and Ohshima et al. [15, 16].

Critical coagulation concentrations of latex particles

Critical coagulation concentrations (CCC) of the various latexes were determined according to the procedure depicted in the experimental part. Due to the thermal-sensitivity of the poly[NIPAM]-rich shell layer, the influence of temperature was examined. Figures 8 and 9 show the variation of the stability ratio (W) as a function of ionic strength (NaCl electrolyte) at 20 and 43 °C, respectively, for three latexes differing in their interfacial structure, i.e., DD1, DD3 and DD11 samples. In addition, the CCC values obtained for all latexes are also given for comparison in Table 3. The general trend is that the obtained CCC values are higher below the LCST than above, irrespective of the latex sample.

At room temperature (Fig. 8 and Table 3), i.e., below the LCST, it is found that the CCC of the various latexes depends upon the type of latex (batch versus shot-growth) and amount of used AEM. It may be postulated that at this temperature, stabilization can be imparted both by electrostatic and steric effects, due to the expansion of the hydrophilic chains constituting the shell layers onto the

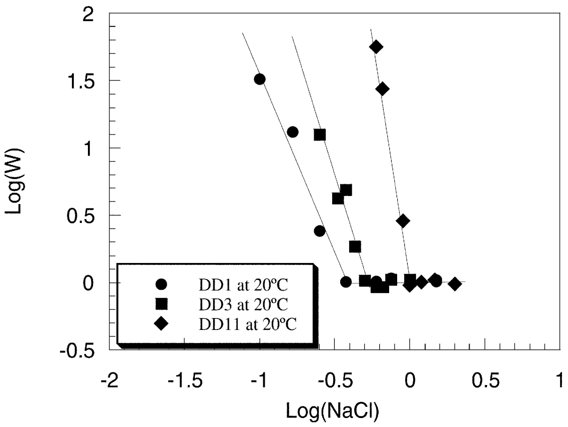

Fig. 8 log–log scale of stability ratio (*W*) of DD1, DD3 and DD11 latexes as a function of the electrolyte (NaCl) concentration (C_s) at 20 °C and pH 6.0

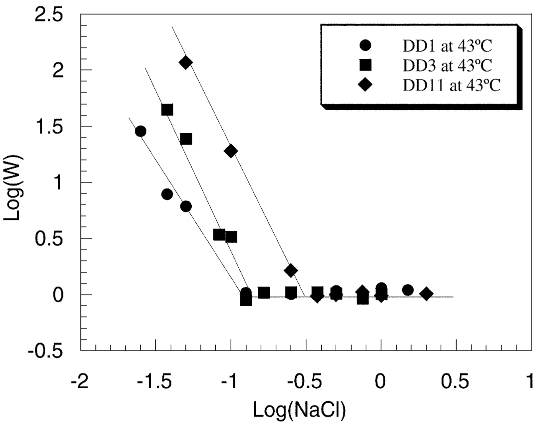

Fig. 9 log–log scale of stability ratio (*W*) as a function of the electrolyte (NaCl) concentration (C_s) of latex particles (run DD1, DD3 and DD11) at 43 °C and pH 6.0

Table 3 Experimental values for CCC at 20 and 43 °C

Sample	CCC [mole/l] at 20 °C	CCC [mole/l] at 43 °C
DD1	0.37	0.12
DD3	0.52	0.13
DD4	0.48	0.17
DD5	0.54	0.14
DD6	0.49	0.14
DD10	0.16	0.04
DD12	0.58	0.17
DD11	1.01	0.34

polystyrene core. The influence of steric stabilization may be emphasized by considering the low CCC values (0.1 to 0.2 mole/l) obtained (at 20 °C) for similarly cationically charged polystyrene latexes [35, 36]. Nevertheless, it should be also remembered that in the case of pure cationic poly[NIPAM] latexes [10] the CCC was of the order of 1 mole/l, due to a large steric barrier (300–500 nm). In the case of the investigated latexes, this barrier, according to thickness data provided in Table 1, is thinner, which may explain the lower CCCs obtained. However, when comparing DD1 and DD10 samples, that only bear cationic charges at chain-ends, the CCCs are 0.37 and 0.16 mole/l, respectively, whereas the corresponding layer thicknesses (Table 1) are 23 and 119 nm. Such a surprising result would probably account for differences in the shell structure in relation with the nature of polymerization process: for DD1 batch sample, poly[NIPAM]-rich hairs would be more flexible than in the case of DD10 sample in which the hydrophilic layer was cross-linked during the shot process, thus reducing the entropic contribution (decrease in the osmotic effect) of the steric stabilization. However, adding more AEM in the shot mixture causes a significant increase in the CCC of the corresponding shot-growth latexes: the larger the ionic charge in the shell layer, the higher the CCC, although the corresponding thickness decreases (down to 21 nm for DD11 sample). This points out the contribution of electrosteric stabilization in the colloidal stability of such latexes.

Above the LCST, the observed strong decrease of the measured CCCs reveals that electrostatic repulsive forces prevail in the particle stabilization mechanism. Some differences are also exhibited according to the type of latex. At first, although both DD1 and DD10 samples (exclusively bear terminal ionic charges), the CCC value drops from 0.12 to 0.04 mole/l, respectively. Such a decrease would again reflect differences in the distribution of ionic charges in the two latexes, a part of them being possibly anchored in the subsurface of the core–shell latex due to the nature of the preparation process. This assumption might be corroborated in considering the slight CCC increase caused upon increasing the concentration of the cationic monomer (DD3–DD6 and DD12 samples). It seems that the observed CCC (0.34 mole/l) is significantly increased only in DD11 sample (which was prepared with the highest amount of AEM).

Conclusions

Cationic amino-containing *N*-isopropylacrylamide–styrene copolymer latexes differing in the preparation process and amount of cationic monomer have been carefully characterized as regards to particle size, surface charge density, electrophoretic mobility and colloidal stability. At first, it was found that the hydrodynamic diameter of all latex particles was found to decrease upon increasing both the salinity of the dispersion medium and the temperature, caused by the increase of the Flory–Huggins interaction parameter and inducing a dehydration process. The presence of the cationic charges did not significantly affect the LCST of the poly[NIPAM]-rich chains although the transition takes place in a broad range of temperature, revealing both the influence of interfacial aspects and compositional gradient profile in such particles.

As expected, both the thermal and electrolyte sensitivity of these latexes was also reflected in their electrophoretic mobility behavior against pH, ionic strength and temperature. The largest effects were found more important with particles exhibiting high cationic charge densities. The relationship between the surface charge density and particle size provided a qualitative explanation however, a complete interpretation of the results cannot actually be proposed due to the complex structure of the shell layer.

Finally, the stability behavior of these latexes against the presence of a monovalent electrolyte was examined below and above the LCST. At room temperature, the latexes were more stable due to repulsive forces imparted, first, by the presence of a steric barrier constituted with the water-swollen shell layer, and second, by electrostatic charges, especially for samples prepared by shot-polymerization process using a cationic monomer. This latter effect only operates above the LCST due to the shrinkage of the shell layer, providing harder particles with cationic charges located at the interface.

Further studies are currently investigated with a view to better understand the electrokinetic properties and stability behaviors of these latexes in the light of recent theories and will be published later on.

References

1. Duracher D, Sauzedde F, Elaïssari A, Perrin A, Pichot C (1998) Colloid Polym Sci 276:219
2. Hoffmann S (1987) J Control Release 6:297
3. Kawaguchi H, Fujimoto K, Mizuhara Y (1992) Colloid Polym Sci 270:53
4. Yoshioka H, Mikami M, Nakai T, Mori Y (1994) Polym Adv Tech 6:418
5. Kondo A, Kaneko T, Higashitani K (1994) Biotech and Bioeng 44:1
6. Kondo A, Kamura H, Higashitani K (1994) Appl Microbiol Biotechnol 41:99
7. Pelton RH, Chibante P (1986) Colloid Surfaces 20:247
8. Mc Phee W, Tam KC, Pelton R (1993) J Colloid Interface Sci 156:24
9. Wu X, Pelton RH, Hamielec AE, Woods DR, McPhee W (1994) Colloid Polym Sci 272:467
10. Meunier F, Elaïssari A, Pichot C (1995) Polym Adv Tech 6:489
11. Pelton RH, Pelton HM, Morphesis A, Rowell RL (1989) Langmuir 5:816
12. Snowden MJ, Vincent B (1992) J Chem Soc Chem Commun 16:1103
13. Fujimoto K, Nakajima Y, Kashiwabara M, Kawaguchi H (1993) Polymer Internat 30:237
14. Ohshima H, Makino K, Kato T, Fujimoto K, Kondo T, Kawaguchi H (1993) J Colloid Interface Sci 159:512
15. Ohshima H (1994) J Colloid Interface Sci 163:474
16. Makino K, Yamamoto S, Fujimoto K, Kawaguchi H, Ohshima HJ (1994) J Colloid Interface Sci 166:251
17. Snowden MJ, Marston NJ, Vincent B (1994) Colloid Polym Sci 272:1273
18. Varoqui R (1982) Nouv J Chim 6:187
19. Tamai H, Hasegawa M, Suzawa T (1989) J Appl Poly Sci 38:403
20. Priest JH, Murray SL, Nelson RJ, Hoffman AS (1987) Reversible Polymeric Gels Related Systems 18:255
21. Chen G, Hoffman (1995) Macromol Rapid Commun 16:175
22. Hiemenz PC (1977) Principles of Colloid and Surface Chemistry. M. Dekker Inc, New York and Basel
23. Ganachaud F, Mouterde G, Delair Th, Elaïssari A, Pichot C (1994) Polym Adv Tech 6:480
24. Hunter R (1981) Zeta Potential in Colloid Science Principles and Applications. Academic Press, New York
25. Kitahara A, Watanabe (1984) Electrical Phenomena at Interfaces, Fundamentals, Measurements, and Application. Marcel Dekker, New York
26. Reerink H, Overbeek JThG (1954) Disc Faraday Soc 18:74
27. Tam KC, Wu XY, Pelton R (1992) Polymer 33:436
28. Kitano H, Kawabata J (1996) Macromol Chem Phys 197:1721
29. Kawaguchi H, Fujimoto K, Mizuhara Y (1992) Colloid Polym Sci 270:53
30. Fujimoto K, Mizuhara Y, Tamura N, Kawaguchi H (1993) J Internat Mat Syst Struct 4:184
31. Seebergh JE, Berg JC (1995) Colloid Surfaces 100:139
32. Sauzedde F, Ganachaud F, Elaïssari A, Pichot C (1997) J Appl Poly Sci 65:2331
33. Van der Lind AJ, Bijsterbosch BH (1990) Croatica Chemica Acta 63:455
34. Hidalgo-Alvarez R, De Las Nieves FJ, Van Der Linde AJ, Bijsterbosch BH (1986) Colloid Surfaces 21:259
35. A. Fernandez-Barbero A, Martin-Rodriguez A, Cellejas-Fernandez J, Hidalgo-Alvarez R (1994) J Colloid Interface Sci 162:257
36. Ganachaud F, Elaïssari A, Pichot C, unpublished data